catalysts

Supplementary Materials: Pyrene-Based Conjugated Polymer/Bi_2MoO_6 Z-Scheme Hybrids: Facile Construction and Sustainable Enhanced Photocatalytic Performance in Ciprofloxacin and Cr(VI) Removal under Visible Light Irradiation

Xianglong Yang [1,2], Yonggang Xiang [1], Xuepeng Wang [1], Shu Li [1], Hao Chen [1,2] and Xing Ding [1,*]

[1] College of Science, Huazhong Agricultural University, Wuhan 430070, China; xianglongyang@foxmail.com (X.Y.); ygxiang@mail.hzau.edu.cn (Y.X.); wangxuepeng@webmail.hzau.edu.cn (X.W.); sueli1301@163.com (S.L.); hchenhao@mail.hzau.edu.cn (H.C.)

[2] Key Laboratory of Environment Correlative Dietology, Ministry of Education, Wuhan 430070, China

* Correspondence: dingx@mail.hzau.edu.cn; Tel.: +86-27-8728 8246

Received: 11 April 2018; Accepted: 27 April 2018; Published: date

1. Preparation of photocatalysts

The Bi_2MoO_6 nanobelts (1BMO) were prepared through the oleyamine-mediated hydrothermal reaction of $Bi(NO_3)_3{\cdot}5H_2O$ and $(NH_4)_6Mo_7O_{24}{\cdot}4H_2O$ [1]. The Bi_2MoO_6 microspheres (3BMO) were prepared using a solvothermal procedure. Typically, $Bi(NO_3)_3{\cdot}5H_2O$ and $Na_2MoO_4{\cdot}2H_2O$ were dissolved in the mixture solution of 7.5mL ethylene glycol (EG) and 45mL ethanol under magnetic stirring. The obtained clear solution was then transferred into a Teflon-lined stainless steel autoclave, and heated at 160 °C for 12 h. The obtained sample was isolated by washing with distilled water, dried in a vacuum oven at 80 °C for 24 h, and then annealed at 350 °C in air atmosphere for 1h. Similar to the synthesis of the Z-scheme hybrids (P-2BMO), the 6.7% P-1BMO and 6.7% P-3BMO hybrids were also fabricated through the in-situ polycondensation of linear pyrene-based conjugated polymer (P17-E) in the presence of Bi_2MoO_6 nanobelts and microspheres, respectively.

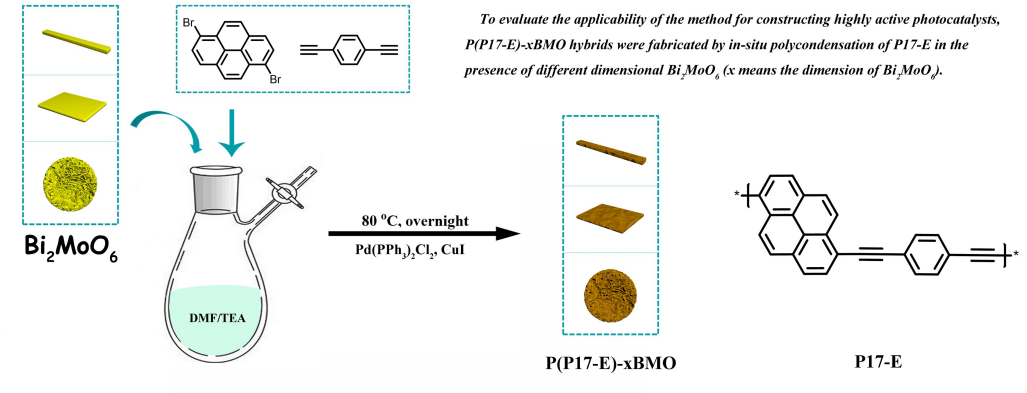

Scheme S1. In situ generation of linear pyrene-based conjugated polymer (P17-E) on the surface of different dimensional Bi_2MoO_6. *N*-Dimethylformamide (DMF); triethylamine (TEA).

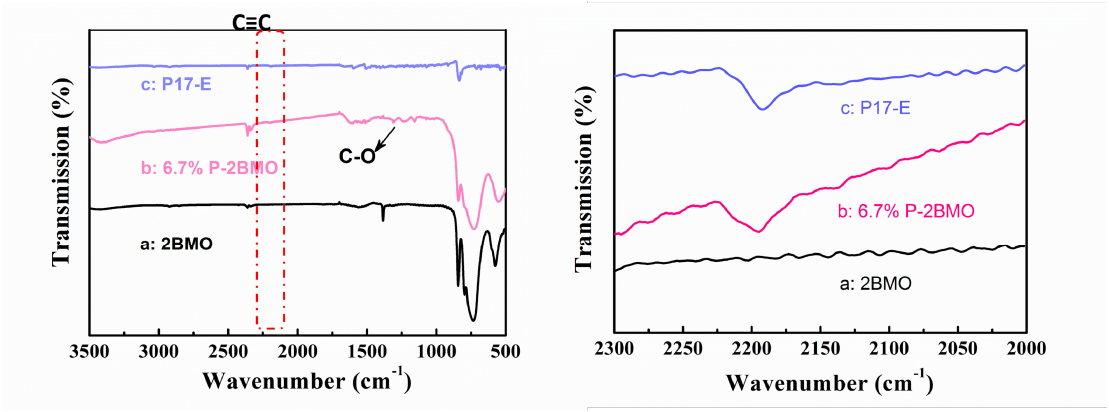

Figure S1. Fourier transform infrared (FT-IR) spectra of 2BMO, 6.7% P-2BMO, and P17-E.

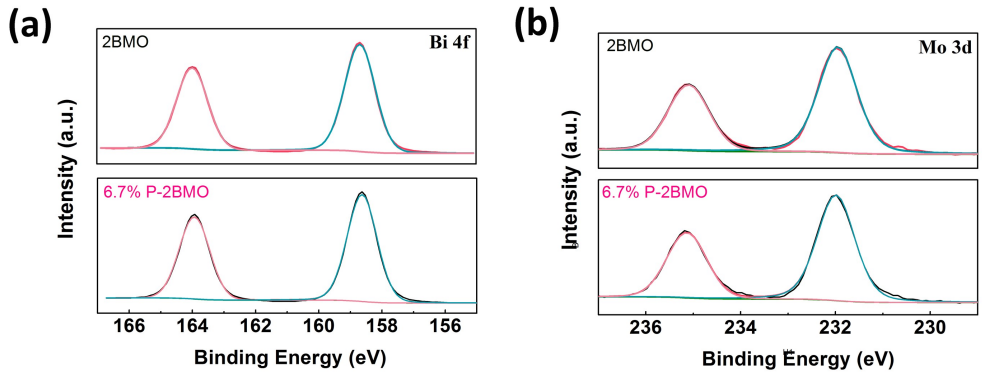

Figure S2. (**a**) X-ray photoelectron spectroscopy (XPS) spectra of Bi 4f and (**b**) Mo 3d.

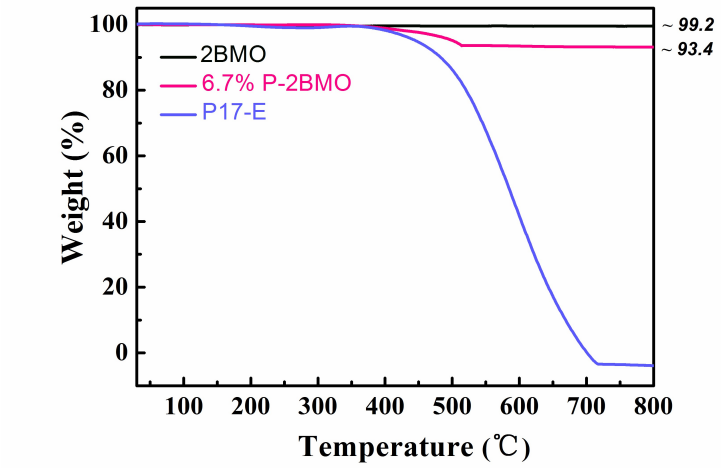

Figure S3. Thermogravimetric (TG) analysis of 2BMO, 6.7% P-2BMO, and P17-E.

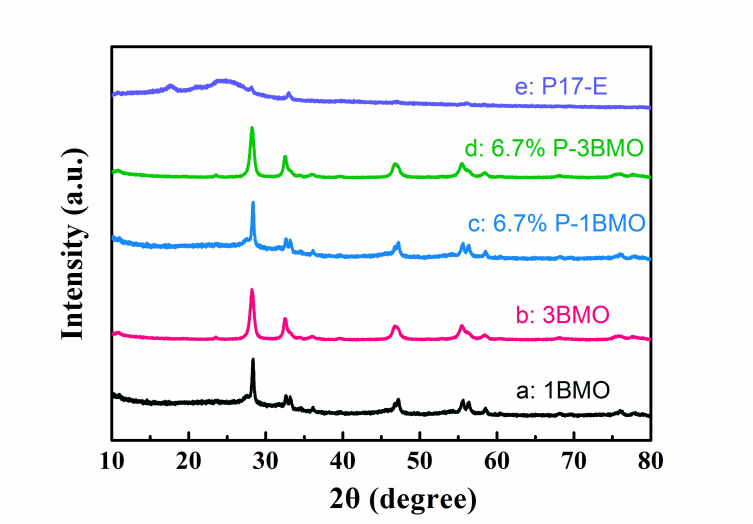

Figure S4. X-ray diffraction (XRD) patterns of 1BMO, 3BMO, 6.7% P-1BMO, 6.7% P-3BMO, and P17-E.

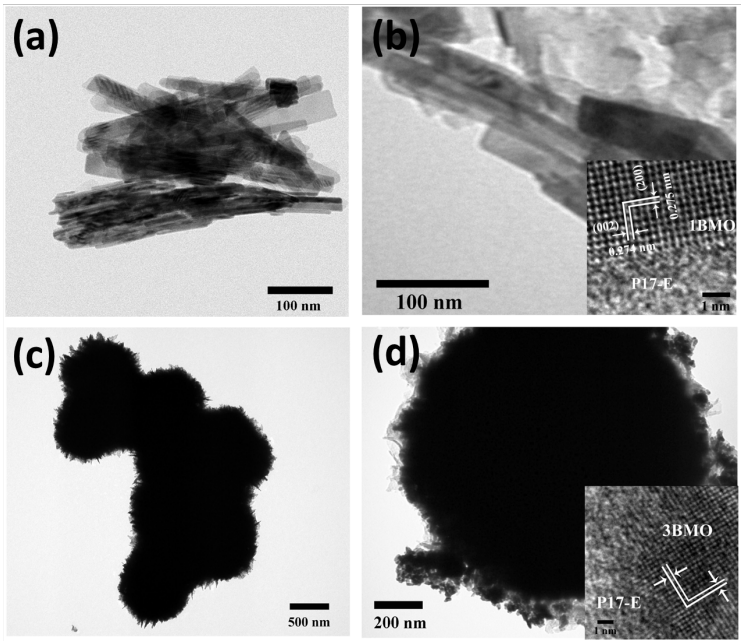

Figure S5. Transmission electron microscopy (TEM) images of 1BMO (**a**), 6.7% P-1BMO (**b**), 3BMO (**c**), and 6.7% P-3BMO (**d**). Inset shows the corresponding high-resolution transmission electron microscopy (HRTEM) images.

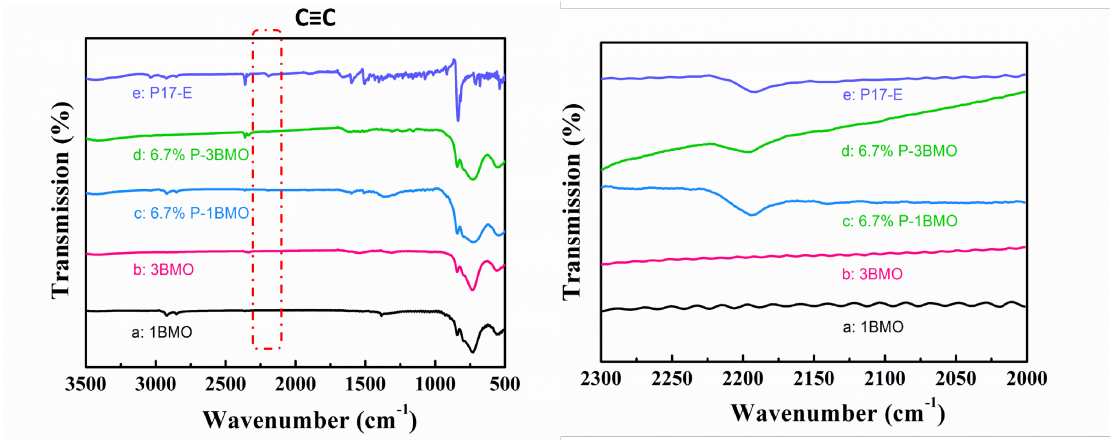

Figure S6. FT-IR spectra of 1BMO, 3BMO, 6.7% P-1BMO, 6.7% P-3BMO, and P17-E.

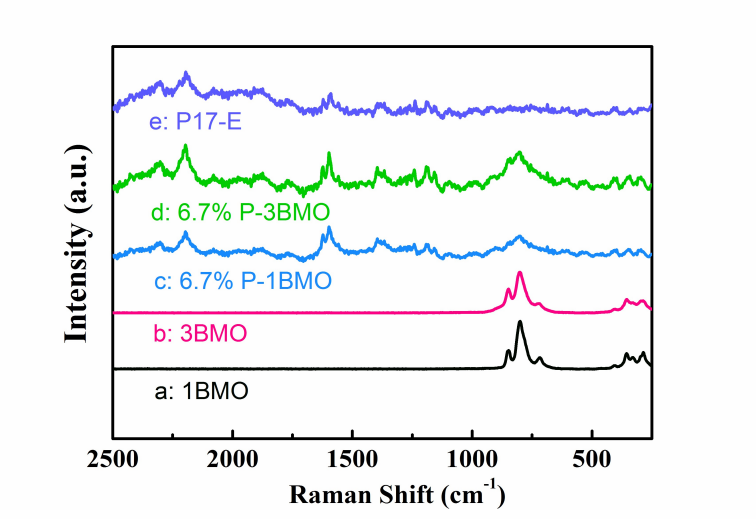

Figure S7. Raman spectra of 1BMO, 3BMO, 6.7% P-1BMO, 6.7% P-3BMO, and P17-E.

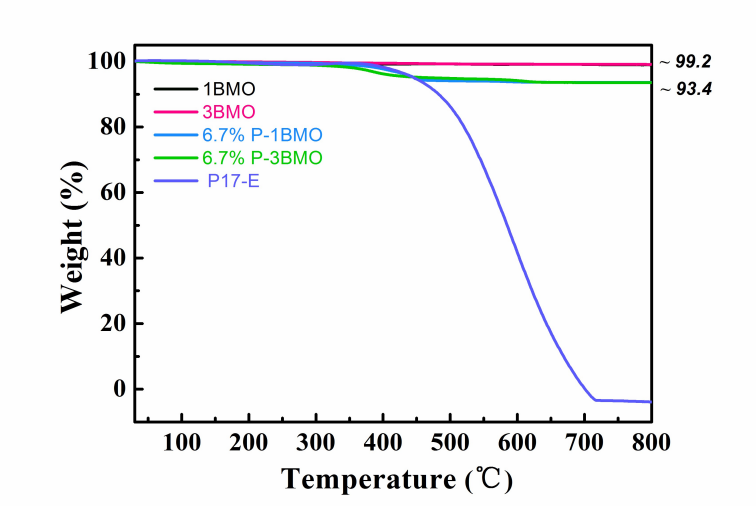

Figure S8. TG analysis of 1BMO, 3BMO, 6.7% P-1BMO, 6.7% P-3BMO, and P17-E.

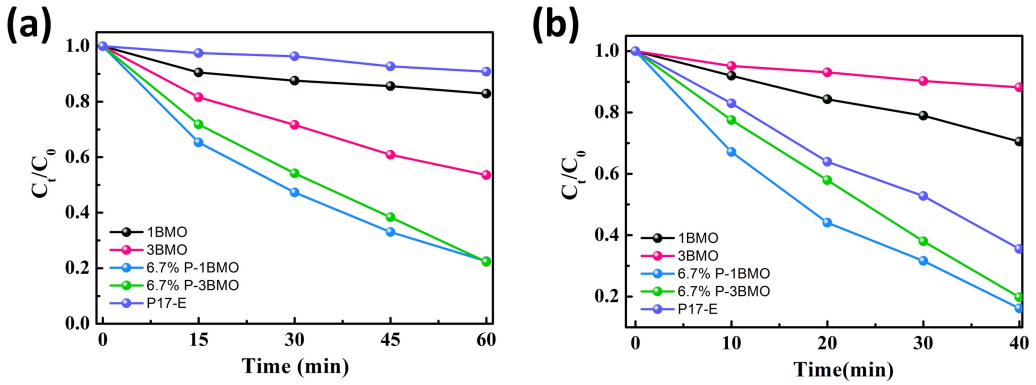

Figure S9. Photodegradation of ciprofloxacin (**a**) and photoreduction of Cr(VI) (**b**) over 1BMO, 3BMO, 6.7% P-1BMO, 6.7% P-3BMO, and P17-E.

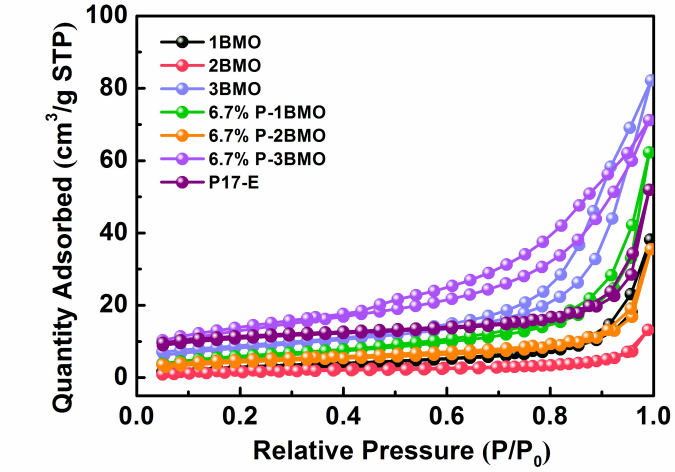

Figure S10. N_2-adsorption–desorption isotherms of all of the samples.

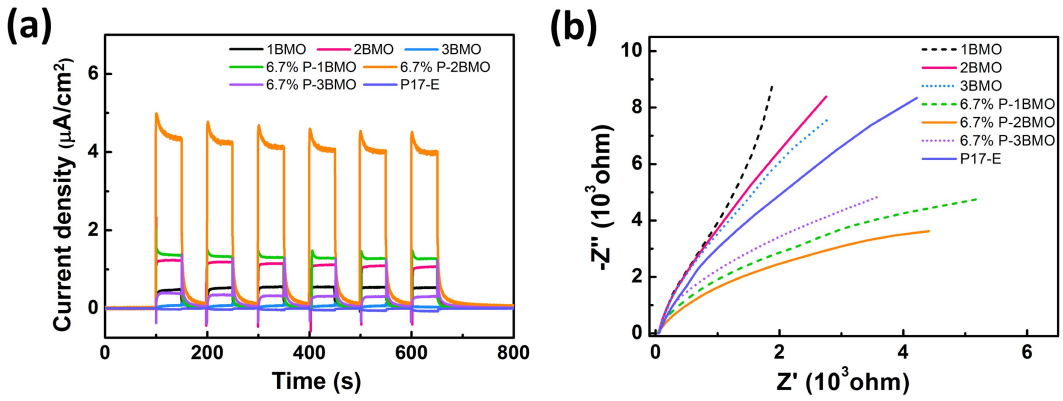

Figure S11. Photocurrent response spectra (**a**) and electrochemical impedance spectra (**b**) of all of the samples.

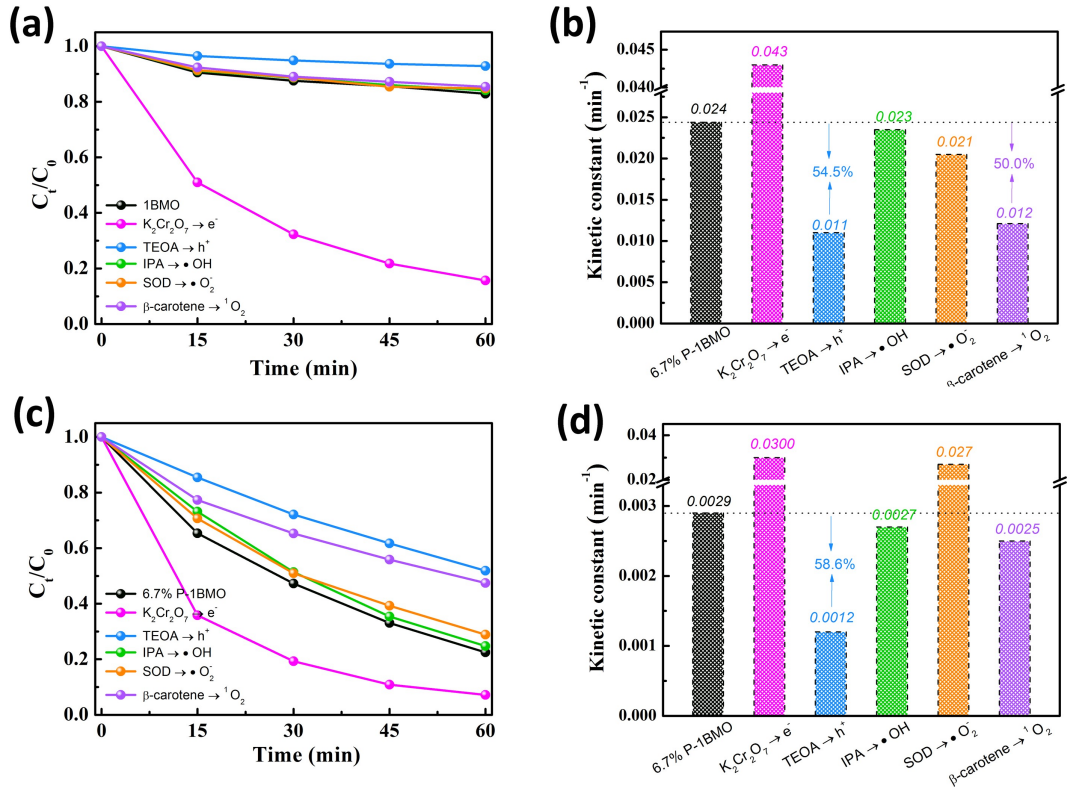

Figure S12. Trapping measurements and the corresponding rate constants for ciprofloxacin photodegradation over 1BMO (**a**, **b**) and 6.7% P-1BMO (**c**, **d**).

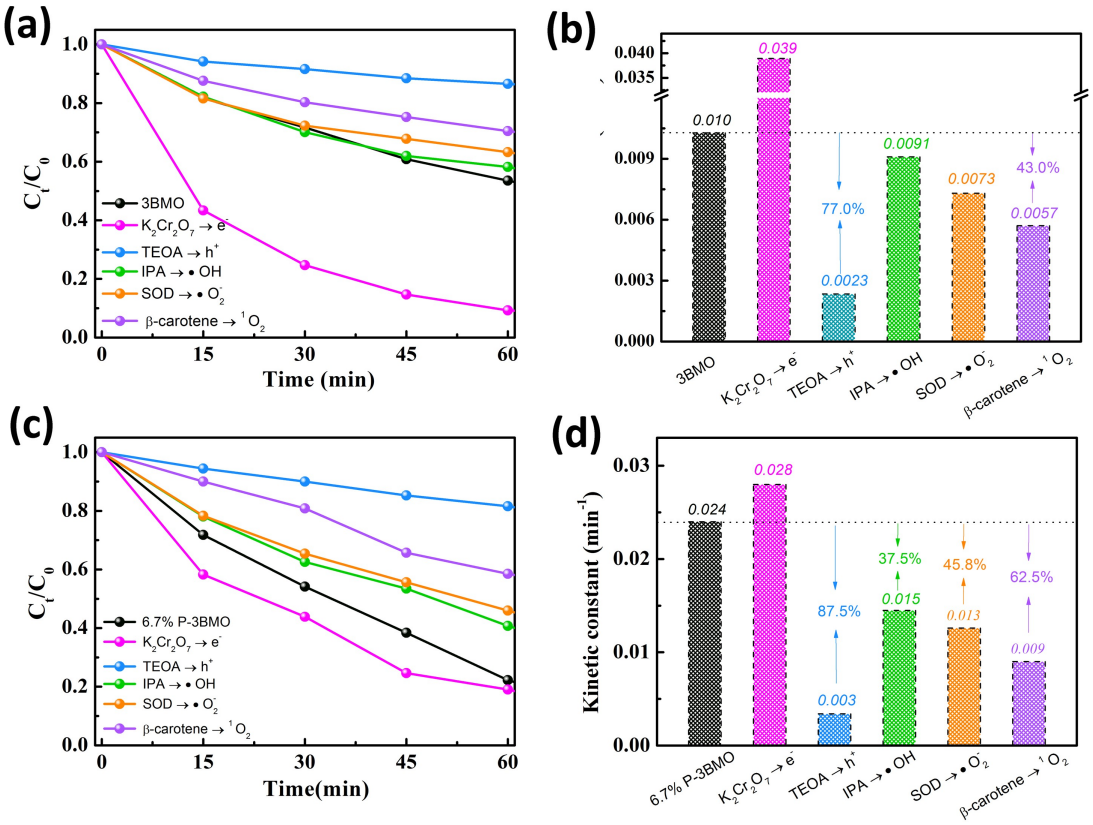

Figure S13. Trapping measurements and the corresponding rate constants for ciprofloxacin photodegradation over 3BMO (**a**, **b**) and 6.7% P-3BMO (**c**, **d**).

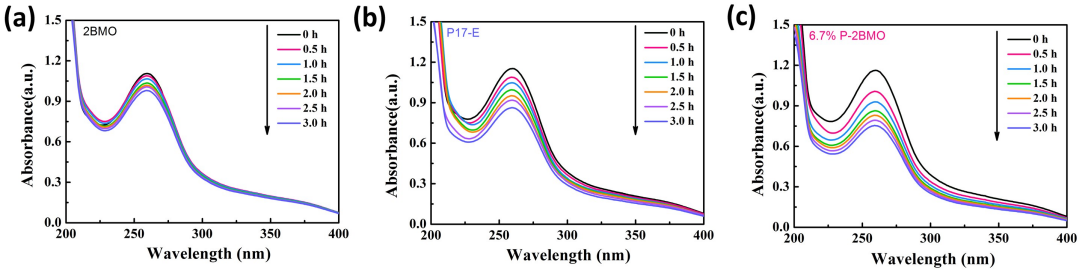

Figure S14. Spectra of the nitroblue tetrazolium (NBT) transformation generated by 2BMO (**a**), P17-E (**b**), and 6.7% P-2BMO (**c**) under visible light irradiation.

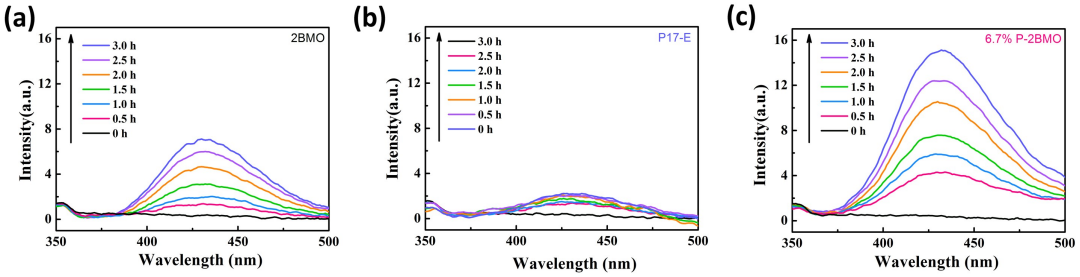

Figure S15. Fluorescence intensity of •OH-trapping photoluminescence (PL) spectra of 2BMO (**a**), P17-E (**b**), and 6.7% P-2BMO (**c**) under visible light irradiation.

Table S1 Comparison of the photodegradation activity. Ciprofloxacin (CIP).

Photocatalyst	Light sources	Catalyst amount	Pollutant	Efficiency	Ref.
g-C_3N_4	$\lambda > 290$ nm	1.0 g/L	4 ppm CIP	100 min for 100%	2
TiO_2	$\lambda > 420$ nm	0.5 g/L	5 ppm CIP	50 min for 98%	3
CQDs/Bi_2WO_6	$\lambda > 400$ nm	0.5 g/L	10 ppm CIP	120 min for 100%	4
CQDs/Bi_2MoO_6	$\lambda > 400$ nm	1.0 g/L	10 ppm CIP	100 min for 90%	5
RGO-$BiVO_4$	$\lambda > 420$ nm	0.2 g/L	10 ppm CIP	40 min for 44%	6
BN/BiOBr	$\lambda > 400$ nm	0.5 g/L	10 ppm CIP	80 min for 80%	7
$Bi_4O_5Br_2$	$\lambda > 400$ nm	0.2 g/L	10 ppm CIP	120 min for 68%	8
BiOBr	$\lambda > 420$ nm	0.2 g/L	5 ppm CIP	120 min for 95%	9
MoS_2/BiOBr	$\lambda > 400$ nm	0.2 g/L	10 ppm CIP	300 min for 88%	10
Bi_2S_3/g-C_3N_4	$\lambda > 420$ nm	0.6 g/L	20 ppm CIP	120 min for 33%	11

Table S2 Brunauer–Emmett–Teller (BET) surface areas of all of the samples. Linear pyrene-based conjugated polymer (P17-E); Z-scheme hybrids (P-BMO).

Sample	1BMO	2BMO	3BMO	6.7%P-1BMO	6.7%P-2BMO	6.7%P-3BMO	P17-E
BET surface (m^2/g)	11.6	6.80	29.2	21.1	15.6	47.3	35.9
Normalized rate (10^{-4} g min^{-1} m^{-2})	2.50	12.9	3.42	11.4	21.8	5.07	0.557

Table S3 The analysis of band positions for 1BMO, 2BMO, and 3BMO. Normal Hydrogen Electrode (NHE); valence band (VB).

Sample	E_f vs. Ag/AgCl (V, pH=7)	E_f vs. NHE (V, pH=0)	CB vs. NHE (V, pH=0)	E_g (eV)	VB vs. NHE (V, pH=0)
1BMO	-0.92	-0.31	-0.41	2.61	2.20
2BMO	-0.87	-0.26	-0.36	2.62	2.26
3BMO	-0.85	-0.24	-0.34	2.63	2.29

References

1. Long, J.; Wang, S.; Chang, H.; Zhao, B.; Liu, B.; Zhou, Y.; Wei, W.; Wang, X.; Huang, L.; Huang, W. Bi_2MoO_6 nanobelts for crystal facet-enhanced photocatalysis. *Small* 2014, *10*, 2791–2795.
2. Wang, F.; Feng, Y.; Chen, P.; Wang, Y.; Su, Y.; Zhang, Q.; Zeng, Y.; Xie, Z.; Liu, H.; Liu, Y.; Lv, W.; Liu, G. Photocatalytic degradation of fluoroquinolone antibiotics using ordered mesoporous g-C_3N_4 under simulated sunlight irradiation: Kinetics, mechanism, and antibacterial activity elimination. *Appl. Catal. B* **2018**, *227*, 114–122.
3. Feng, X.; Wang, P.; Hou, J.; Qian, J.; Ao, Y.; Wang, C. Significantly enhanced visible light photocatalytic efficiency of phosphorus doped TiO_2 with surface oxygen vacancies for ciprofloxacin degradation: Synergistic effect and intermediates analysis. *J. Hazard. Mater.* **2018**, *351*, 196–205.
4. Di, J.; Xia, J. ; Ge, Y. ; Li, H.; Ji, H.; Xu, H.; Zhang, Q. ; Li, H.; Li, M. Novel visible-light-driven CQDs/Bi_2WO_6 hybrid materials with enhanced photocatalytic activity toward organic pollutants degradation and mechanism insight. *Appl. Catal. B* **2015**, *168*, 51–61.
5. Di, J.; Xia, J.; Ji, M.; Li, H.; Xu, H.; Li, H.; Chen, R. The synergistic role of carbon quantum dots for the improved photocatalytic performance of Bi_2MoO_6. *Nanoscale.* **2017**, *7*, 11433–11443.
6. Yan, Y.; Sun, S.; Song, Y.; Yan, X.; Guan, W.; Liu, X.; Shi, W. Microwave-assisted in situ synthesis of reduced graphene oxide-$BiVO_4$ composite photocatalysts and their enhanced photocatalytic performance for the degradation of ciprofloxacin. *J. Hazard. Mater.* **2013**, *250*, 106–114.
7. Di, J .; Xia, J.; Ji, M.; Wang, B.; Yin, S.; Zhang, Q.; Chen, Z.; Li, H. Advanced photocatalytic performance of graphene-like BN modified BiOBr flower-like materials for the removal of pollutants and mechanism insight. *Appl. Catal. B* **2016**, *183*, 254–262.
8. Di, J.; Xia, J.; Ji, M.; Yin, S.; Li, H.; Xu, H.; Zhang, Q.; Li, H. Controllable synthesis of $Bi_4O_5Br_2$ ultrathin nanosheets for photocatalytic removal of ciprofloxacin and mechanism insight. *J. Mater. Chem. A* **2015**, *3*, 15108–15118.
9. Zhang, X.; Li, R.; Jia, M.; Wang, S.; Huang, Y.; Chen, C. Degradation of ciprofloxacin in aqueous bismuth oxybromide (BiOBr) suspensions under visible light irradiation: A direct hole oxidation pathway. *Chem. Eng. J.* **2015**, *274*, 290–297.
10. Xia, J.; Ge, Y.; Zhao, D.; Di, J.; Ji, M.; Yin, S.; Li, H.; Chen, R. Microwave-assisted synthesis of few-layered MoS_2/BiOBr hollow microspheres with superior visible-light-response photocatalytic activity for ciprofloxacin removal. *Cryst.Eng.Comm* **2015**, *17*, 3645–3651.
11. Zhu, C.; Gong, T.; Xian, Q.; Xie, J. Graphite-like carbon nitride coupled with tiny Bi_2S_3 nanoparticles as 2D/0D heterojunction with enhanced photocatalytic activity. *Appl. Surf. Sci.* **2019**, *444*, 75–86.